12th IFAC International Symposium on
Advanced Control of Chemical Processes
July 14-17, 2024. Toronto, Canada

Spatial State Profile Estimation in Tubular Reactor Systems in Presence of Bound Constraints

Gaurav Seth[a], **Mani Bhushan**[a] *, **Sachin C. Patwardhan**[a]

[a] *Department of Chemical Engineering, IIT Bombay, Powai, Mumbai-400076, India.*

Abstract: Designing state estimation strategies for discrete time nonlinear dynamic systems often requires incorporation of inequality constraints on the state estimates. These constraints may arise from physical considerations and/or operational perspective which can significantly increase the complexity of the estimator design problem. The estimation problem becomes even more challenging for distributed parameter systems (DPSs) due to spatial dependency of the system states. This paper provides two novel approaches for estimating the state profiles of DPSs while adhering to the imposed bounds. The first approach utilizes the idea of constraining the maximum and minimum values that spatial state profiles can take along the spatial domain. The second approach employs a characteristic property of Bernstein polynomials to achieve state profile estimates within the specified bounds. Proposed approaches are compared with an existing approach that incorporates bound constraints at a large number of discretization points. However, it does not guarantee constraint satisfaction by the entire profile. The performance of the proposed approaches is evaluated by simulation studies conducted on an auto-thermal tubular reactor system. The analysis of the estimation results demonstrates that the proposed approaches are capable of producing accurate profile estimates within the specified bounds.

Keywords: Profile Constraints, Distributed Parameter System, DAE-EKF

1. INTRODUCTION

Numerous engineering applications such as plug flow reactors and packed-bed reactors are based on the transport reaction processes. The process variables in such systems depend on the temporal as well as spatial coordinates. Modeling and analysis of such systems, also known as distributed parameter systems (DPSs), involves representing the systems using partial differential equations (PDEs) (Yupanqui Tello et al. (2021)). Given the spatial dependency of the process variables of DPSs coupled with availability of typically a limited number of spatially distributed measurements, the online state estimation of multispecies transport reaction systems is a challenging task. Over the years, various approaches have been proposed for the same. Model order reduction or early lumping based approaches are widely used in literature for designing state estimators for DPSs (Marko et al. (2018)). Orthogonal collocation (OC) is a popoular method of model order reduction. The resulting reduced-dimension model represented by a set of differential-algebraic equations (DAE) can then be combined with any Bayesian estimator (e.g. extended Kalman filter (EKF)) or Luenberger observer to estimate the states of the system. The advantage of using OC method based on an interpolating polynomial is the ability to generate polynomial approximation of the spatial state profiles of the system (Seth et al. (2023)).

The states of a DPS also often satisfy some constraints arising from physical laws (such as non-negativity of concentrations), or from operational considerations. However, the state estimates obtained from a Bayesian estimator may violate these constraints. A straightforward approach to prevent the violation of constraints can be to make use of the constrained state estimation approach as proposed in the literature for lumped parameter systems (Mandela et al. (2010), Pacharu et al. (2012)). However, integrating the constrained estimation technique along with reduced dimension OC model guarantees the constraints satisfaction only at discrete collocation points and is not sufficient for ensuring constraints satisfaction throughout the spatial profile (Seth et al. (2023)). Recently, Seth et al. (2023) proposed an alternate method where they imposed constraints on the states at large number of spatially discertized points (and not just collocation points) during state estimation. However, this approach also does not guarantee constraint satisfaction at spatial points other than the discretized points. Also, ensuring constraints satisfaction at large number of points can lead to increased computational complexity during online state estimation which is undesirable.

In the current work, we propose two alternate analytical methods for ensuring bound constraints on the estimated spatial state profiles of a DPS. The proposed approaches eliminate the need for spatial discretization of the state profiles while guaranteeing constraint satisfaction throughout the spatial profile. Both the approaches utilize a key feature of the OC approach, namely the representation of state profiles as polynomial approximations at any given time instant. The first approach finds and constraints

* Corresponding author (e-mail: mbhushan@iitb.ac.in)

the minimum and maximum values of the polynomial to be within bounds. These extreme values are in-turn obtained by obtaining roots of the derivative polynomial. The second approach involves expressing the state profile polynomial as a Bernstein polynomial (BP). It then uses a key property of BP that maximum and minimum values of a BP are bounded by the maximum and minimum of the corresponding BP coefficients (Lane and Riesenfeld (1981)). Thus, ensuring that BP coefficients are within bounds, ensures that estimated state profile satisfies the bounds. The efficacy of the proposed approaches is demonstrated via simulation studies on an auto-thermal tubular reactor system (Berezowski et al. (2000)).

The rest of the paper is organized as follows: Section 2 gives the details of process models. Section 3 discusses the proposed analytical approaches for ensuring profile constraints. Section 4 presents the simulation based results. Final conclusions are drawn in Section 5.

2. PRELIMINARIES

2.1 Process model

A general nonlinear DPS in one dimension can be represented by a set of PDEs given by Eq. (1), where $z \in [0,1]$ denotes the spatial domain, $t \in [0, \infty)$ denotes the temporal domain and x_r $(r = 1, 2, ..., n)$ denotes the dependent r^{th} state variable of the system.

$$\frac{\partial x_r(z,t)}{\partial t} = f_r\left(\frac{\partial x_r(z,t)}{\partial z}, \frac{\partial^2 x_r(z,t)}{\partial z^2}, \mathbf{x}(z,t), \mathbf{m}(t), z\right) \tag{1}$$

The boundary conditions and initial conditions associated with the system can be given by Eqs. (2 - 4)

$$g_r\left[\frac{dx_r}{dz}, \mathbf{x}(0,t)\right] = 0 \qquad \text{at } z = 0 \tag{2}$$

$$h_r\left[\frac{dx_r}{dz}, \mathbf{x}(1,t)\right] = 0 \qquad \text{at } z = 1 \tag{3}$$

$$x_r(z,0) = a_r(z) \tag{4}$$

Here, $\mathbf{x} = [x_1, ..., x_r, ..., x_n]^T$ is the combined state vector, $\mathbf{m}(t) \in \mathbb{R}^{m\times 1}$ denotes the vector of manipulated inputs in the plant. Here, we intend to study the dynamics of DPS by employing a computer controlled system. Let $t_k = kT_s : k = 1, 2, ...$ represent the sampling instants with T_s as the sampling interval. Variation of manipulated inputs is assumed to follow a zero-order hold behaviour for $t \in [kT_s, (k+1)T_s)$.

2.2 Reduced Dimensional Model

This section presents a brief formulation of lower dimensional DAE model using OC technique (Gupta (1995)). First and second order derivatives in the PDE system (Eqs. (1) to (3)) are approximated using N^{th} order Lagrange interpolating polynomial at the chosen $N+1$ collocation points (ξ_j). The collocation points are such that $\xi_1 = 0, \xi_{N+1} = 1$ and the set of intermediate points $\boldsymbol{\xi} \triangleq \{\xi_j\}_{j=2}^{N}$ lie at the roots of shifted Legendre polynomial. Further, defining the values for r^{th} state variable at j^{th} collocation point and k^{th} sampling instant as $\chi_{r,j}(k) \triangleq \chi_r(\xi_j, k)$, vectors of differential and algebraic states can be written as $\boldsymbol{\chi}_r^d(k) = [\chi_{r,2}(k), ..., \chi_{r,N}(k)]_{(N-1)\times 1}^T$ and $\boldsymbol{\chi}_r^a(k) = [\chi_{r,1}(k)\ \chi_{r,N+1}(k)]_{2\times 1}^T$. Further, stacking the differential and algebraic states for all the n state variables yield $\boldsymbol{\chi}^d(k) = \left[\left(\boldsymbol{\chi}_1^d(k)\right)^T, ..., \left(\boldsymbol{\chi}_n^d(k)\right)^T\right]_{n_d\times 1}^T$ and $\boldsymbol{\chi}^a(k) = \left[\left(\boldsymbol{\chi}_1^a(k)\right)^T, ..., \left(\boldsymbol{\chi}_n^a(k)\right)^T\right]_{n_a\times 1}^T$, where $n_d = n(N-1)$ and $n_a = 2n$. Using these definitions and applying OC technique a reduced dimension discrete time DAE model is obtained. Further, the DAE model was compensated for model plant mismatch (MPM) arising due to model order reduction of original PDE system (Seth et al. (2023)). The MPM signal was assumed to behave as an additive zero mean Gaussian signal i.e., $\mathbf{w}_a(k) \sim \mathcal{N}(\mathbf{0}_{n_d\times 1}, \mathbf{Q}_a)$. The state dynamics including $\mathbf{w}_a(k)$ can be represented as

$$\boldsymbol{\chi}^d(k+1) = \mathbf{F}(\boldsymbol{\chi}^d(k), \boldsymbol{\chi}^a(k), \mathbf{m}(k), \boldsymbol{\xi}) + \mathbf{w}_a(k) \tag{5}$$

$$\mathbf{0}_{n_a\times 1} = \boldsymbol{\Lambda}(\boldsymbol{\chi}^d(k+1), \boldsymbol{\chi}^a(k+1)) \tag{6}$$

where,

$$\mathbf{F}(.) = \boldsymbol{\chi}^d(k) + \int_{kT_s}^{(k+1)T_s} \mathcal{F}(\boldsymbol{\chi}^d(t), \boldsymbol{\chi}^a(t), \mathbf{m}(k), \boldsymbol{\xi})dt \tag{7}$$

Here, $\mathcal{F}$ represents a stacked function vector of n_d ODEs, $\boldsymbol{\Lambda}$ represents a vector of n_a algebraic equations. The true values of manipulated inputs are assumed to vary as $\mathbf{m}(k) = \mathbf{u}(k) + \mathbf{w}_u(k)$, where $\mathbf{u}(k)$ is the computer/operator defined input and $\mathbf{w}_u(k)$ is a zero mean Gaussian white noise signal such that $\mathbf{w}_u(k) \sim \mathcal{N}(\mathbf{0}_{m\times 1}, \mathbf{Q}_u)$. Vectors $\boldsymbol{\chi}^d(k)$ and $\boldsymbol{\chi}^a(k)$ are combined to form the augmented state vector $\boldsymbol{\chi}(k) \in \mathbb{R}^{n(N+1)\times 1}$. Similar to the state dynamics, effect of MPM ($\mathbf{v}_a(k)$) was also introduced in the measurement model which can be represented as

$$\mathbf{Y}(k+1) = \mathbf{C}_m\boldsymbol{\chi}(k+1) + \mathbf{v}(k+1) \tag{8}$$

Here, $\mathbf{v}(k) = \mathbf{v}_s(k) + \mathbf{v}_a(k) \sim \mathcal{N}(\mathbf{0}_{\eta\times 1}, \mathbf{R})$ and $\mathbf{R} = (\mathbf{R}_s + \mathbf{R}_a)_{\eta\times\eta}$, where, $\mathbf{v}_s(k)$ represent the sensor noise which is assumed to be zero mean white noise signal with known density i.e., $\mathbf{v}_s(k) \sim \mathcal{N}(\mathbf{0}_{\eta\times 1}, \mathbf{R}_s)$, where η is the total number of measurements for all the n state variables. Further, $\mathbf{C}_m$ is formulated using Lagrange polynomials evaluated at the measurement locations (Seth et al. (2023)). The formulated measurement matrix thus allows to systematically relate the states obtained at the collocation points to the state values at the measurement locations anywhere in the spatial domain of the system.

Note that the resulting measurement and state noises ($\mathbf{w}_a(k)$ and $\mathbf{v}(k)$) are identified to be correlated with the cross-correlation matrix, $\mathbf{S}$. The details on quantification of $\mathbf{Q}_a, \mathbf{R}_a$, and $\mathbf{S}$ are given in Seth et al. (2023). Further, utilizing the state vector, $\boldsymbol{\chi}(k)$ containing the state values only at collocation points, the reconstructed state profiles can be obtained as

$$\chi_r(z,k) = \left[\mathbf{L}^d(z)\right]^T \boldsymbol{\chi}_r^d(k) + \left[\mathbf{L}^a(z)\right]^T \boldsymbol{\chi}_r^a(k) \tag{9}$$
$$r = 1, 2, ..., n \text{ and } z \in [0,1]$$

where, $\mathbf{L}^d(z)$ and $\mathbf{L}^a(z)$ are the vectors of Lagrange basis polynomials ($L_j(z) : j = 1, 2, ..., N+1$) formed at internal collocation points and the boundary points. The definition of Lagrange basis polynomials and their derivatives can be referred from Seth et al. (2023). Each of these functions ($\chi_r(z,k)$) characterize a spatial state profile of the system constructed over the entire spatial domain.

2.3 DAE-EKF (Seth et al. (2023))

A brief review of the steps involved in the unconstrained EKF for DAE systems (Eqs. (5) to (8)) with correlated state and measurement noise (Seth et al. (2023)) is now presented. Given the estimated states, $\widehat{\boldsymbol{\chi}}(k|k)$ at k^{th} sampling instant and the combined covariance matrix, $\mathbf{P}(k|k)$, the method consists of twe steps:

(1) Prediction step:

$$\widehat{\boldsymbol{\chi}}^d(k+1|k) = \mathbb{F}(\widehat{\boldsymbol{\chi}}(k|k), \mathbf{u}(k), \boldsymbol{\xi}, \mathbf{S}, \mathbf{R}, \mathbf{Y}(k)) \tag{10}$$

$$\mathbf{0}_{2n\times 1} = \boldsymbol{\Lambda}(\widehat{\boldsymbol{\chi}}^d(k+1|k), \widehat{\boldsymbol{\chi}}^a(k+1|k)) \tag{11}$$

$$\mathbf{P}(k+1|k) = \boldsymbol{\Upsilon}(\widehat{\boldsymbol{\chi}}(k|k), \mathbf{P}(k|k), \mathbf{u}(k), \mathbf{Q}_u, \mathbf{Q}_a, \mathbf{S}, \mathbf{R}) \tag{12}$$

Note that the terms $\mathbf{S}, \mathbf{R}$ and $\mathbf{Y}(k)$ have been retained in the prediction step to emphasize that $\mathbf{S}, \mathbf{R}$ and $\mathbf{Y}(k)$ may explicitly be used in the prediction step.

(2) Unconstrained Update step:

$$\widehat{\boldsymbol{\chi}}^d(k+1|k+1) = \boldsymbol{\Psi}(\widehat{\boldsymbol{\chi}}(k+1|k), \mathbf{P}(k+1|k), \mathbf{R}, \mathbf{Y}(k+1)) \tag{13}$$

$$\mathbf{P}(k+1|k+1) = \boldsymbol{\Pi}(\widehat{\boldsymbol{\chi}}(k+1|k), \mathbf{P}(k+1|k), \mathbf{R}, \mathbf{Y}(k+1)) \tag{14}$$

Here, $\mathbb{F}(.)$ and $\boldsymbol{\Upsilon}(.)$ represent the prediction steps and $\boldsymbol{\Psi}(.)$ and $\boldsymbol{\Pi}(.)$ represent the update steps respectively. The updated algebraic states can be evaluated using Eq. (11). Further, updated state vector obtained from DAE-EKF is transformed to achieve continuous functions ($\widehat{\chi}_r(z,k)$: $r = 1, ..., n$ and $z \in [0,1]$) using Eq. (9).

3. PROBLEM STATEMENT AND RELEVANT CONSTRAINED ESTIMATION APPROACH

3.1 Problem Statement

Let us assume that at $(k+1)^{th}$ sampling instant the plant state profiles are bounded by lower and upper bounds as

$$x_{r,L} \leq x_r(z, k+1) \leq x_{r,H} \tag{15}$$
$$r = 1, 2, ..., n \text{ and } \forall z \in [0,1]$$

where, $x_r(z, k+1)$ is the plant state profile for the r^{th} state variable and $x_{r,L}$ and $x_{r,H}$ represent the known lower and upper bounds. In this work we propose to develop constrained profile estimation schemes for DPSs using a reduced dimension OC model. Therefore, it is crucial to express the constraints given by Eq. (15) in terms of the state values obtained from the OC model. This can be achieved by using the reconstructed state profile obtained using OC states along with the Lagrange polynomial. Thus, using the reconstructed state profiles Eq. (15) can be recasted as

$$x_{r,L} \leq \chi_r(z, k+1) \leq x_{r,H} \tag{16}$$
$$r = 1, 2, ..., n \text{ and } \forall z \in [0,1]$$

Further, stacking for all the state variables we get:

$$\mathbf{X}_L \leq \boldsymbol{\chi}(z, k+1) \leq \mathbf{X}_H \quad \forall z \in [0,1] \tag{17}$$

where, $\boldsymbol{\chi}(z, k+1) = [\, \chi_1(z, k+1) \;...\; \chi_n(z, k+1) \,]^T$,

$$\mathbf{X}_L = [\, x_{1,L} \;...\; x_{n,L} \,]^T \text{ and } \mathbf{X}_H = [\, x_{1,H} \;...\; x_{n,H} \,]^T$$

Thus, at $(k+1)^{th}$ sampling instant, the constrained profile estimation problem is to obtain the estimated state vector $\widehat{\boldsymbol{\chi}}(k+1|k+1)$ such that the state profile estimates, $\widehat{\chi}_r(z, k+1)$ for $r = 1, 2, ..., n$ and $\forall z \in [0,1]$ are bounded by their respective lower and upper bounds. Using Eq. (17) the constrained update step can be formulated to solve the following optimization problem which can be considered as an extended version of the recursive nonlinear data reconciliation (RNDDR) technique given by Mandela et al. (2010). This extension is designed for enforcing profile constraints and can be formulated as

$$\widehat{\boldsymbol{\chi}}(k+1|k+1) = \underset{\boldsymbol{\chi}(k+1)}{\operatorname{argmin}}\big((\boldsymbol{\varepsilon}^d(k+1))^T \left(\mathbf{P}^d(k+1|k)\right)^{-1}$$
$$\boldsymbol{\varepsilon}^d(k+1)) + ((\mathbf{Y}(k+1) - \mathbf{C}_m\boldsymbol{\chi}(k+1))^T$$
$$\mathbf{R}^{-1}\left(\mathbf{Y}(k+1) - \mathbf{C}_m\boldsymbol{\chi}(k+1)\right)\big)) \tag{18}$$

subject to

$$\mathbf{0}_{2n\times 1} = \boldsymbol{\Lambda}(\boldsymbol{\chi}^d(k+1), \boldsymbol{\chi}^a(k+1)) \tag{19}$$

$$\mathbf{X}_L \leq \boldsymbol{\chi}(z, k+1) \leq \mathbf{X}_H \quad \forall z \in [0,1] \tag{20}$$

Here, $\boldsymbol{\varepsilon}^d(k+1) = \boldsymbol{\chi}^d(k+1) - \widehat{\boldsymbol{\chi}}^d(k+1|k)$, and $\mathbf{P}^d(k+1|k)$ are prediction errors and covariance matrix of differential states at $(k+1)^{th}$ instant. Further, Eq. (19) refers to the algebraic equations of the system, Eq. (20) represents the desired bounds on the state profiles of the system. Solving the optimization problem given by Eqs. (18-20) is a challenging problem since ensuring constraints on the entire spatial domain ($z \in [0,1]$) is not straightforward and may require some numerical techniques or manipulations.

3.2 Constrained Update step - Discretization Approach (Seth et al. (2023)):

One simple numerical technique proposed by Seth et al. (2023) involves approximating the profile constraints through a large number of linear inequality constraints. These constraints essentially bound the individual state values evaluated at a large number of evenly spaced grid points in space. Thus, the profile constraint (Eq. (20)) was replaced by the constraints given as (Seth et al. (2023)):

$$\mathbb{X}_L \leq \boldsymbol{\chi}(\mathcal{Z}, k+1) \leq \mathbb{X}_H \tag{21}$$

where $\mathcal{Z} \triangleq \{z_i\}_{i=1}^{N_c}$ is set of equidistant grid points chosen for imposing the constraints. Note that number of grid points (N_c) required for imposing profile constraint is typically very large compared to the number of collocation points used for developing OC model i.e., $N_c >> N$. Here $\boldsymbol{\chi}(\mathcal{Z}, k+1)$ represents a vector of state values evaluated at the points contained in the set $\mathcal{Z}$, i.e.,

$$\boldsymbol{\chi}(\mathcal{Z}, k+1) = \left[\, (\boldsymbol{\chi}_1(\mathcal{Z}, k+1))^T \;...\; (\boldsymbol{\chi}_n(\mathcal{Z}, k+1))^T \,\right]^T \tag{22}$$

where $\boldsymbol{\chi}_r(\mathcal{Z}, k+1) = \left[\, \chi_{r,z_1}(k+1) \;...\; \chi_{r,z_{N_c}}(k+1) \,\right]^T$. Additionally, $\mathbb{X}_L$ and $\mathbb{X}_H$ are defined as

$$\mathbb{X}_L = \left[\, (x_{1,L})\, \mathbf{1}^{N_c+1} \;\cdots\; (x_{n,L})\, \mathbf{1}^{N_c+1} \,\right]^T$$
$$\mathbb{X}_H = \left[\, (x_{1,H})\, \mathbf{1}^{N_c+1} \;\cdots\; (x_{n,H})\, \mathbf{1}^{N_c+1} \,\right]^T \tag{23}$$

Here, $\mathbf{1}^{N_c+1}$ represents row vector of ones of size $(N_c + 1)$. Using large value of N_c may result in bounded state profile estimates, however, imposing constraints on large number of grid points does not give a formal guarantee that states at other locations will also satisfy the constraints. Additionally the computational complexity of the problem also increases with increasing, N_c i.e., increasing the number of constraints. For the special case of linear algebraic equations (Eq. (19)), constrained updated step optimization problem becomes a quadratic programming (QP) problem.

4. PROPOSED APPROACHES

4.1 Using Extremum of the State Profiles

One fundamental approach to obtain bounded state profile estimates is to bound its maximum and minimum values within the specified range. Consider the spatial state profile function for the r^{th} state variable at k^{th} sampling instant, $\chi_r(z,k)$. Extreme values of $\chi_r(z,k)$ can be identified by locating the roots of its derivative $\chi\prime_r(z,k)$. Note that the function $\chi\prime_r(z,k)$ may have complex roots or roots outside the considered spatial domain. We thus define a set of real roots within the spatial domain of interest as $\mathrm{z}_r(k) \triangleq \{z_{r,i} : z_{r,i} \in \mathbb{R}, z_{r,i} \in [0,1]$ and $\chi\prime_r(z_{r,i},k) = 0$ for $i = 1,...,n_{r,k}\}$. Here, $n_{r,k}$ is the number of locations displaying extreme values of r^{th} state profile obtained at k^{th} sampling instant. The maximum/minimum value that $\chi_r(z,k)$ can attain $\forall\ z \in [0,1]$ corresponds to the maximum/minimum value it can achieve at the locations contained in set $\mathrm{z}_r(k)$, i.e.,

$$\chi_{r,\max}(k) \triangleq \max_{z\in[0,1]}(\chi_r(z,k)) = \max_{z\in \mathrm{z}_r(k)}(\chi_r(z,k)) \quad (24)$$

$$\chi_{r,\min}(k) \triangleq \min_{z\in[0,1]}(\chi_r(z,k)) = \min_{z\in \mathrm{z}_r(k)}(\chi_r(z,k)) \quad (25)$$

where, $\chi_{r,\max}(k)$ and $\chi_{r,\min}(k)$ are the extreme values that the profile function $\chi_r(z,k)$ can attain at k^{th} sampling instant. Hence, by specifying the bounds on $\chi_{r,\max}(k)$ and $\chi_{r,\min}(k)$, the profile of the r^{th} state variable can be restricted to stay within the specified bounds. Similar computations can be carried out for all the n state variables. The maximum and minimum values of all the state variables can then be stacked to form vectors $\boldsymbol{\chi}_{\max}(k)$ and $\boldsymbol{\chi}_{\min}(k) \in \mathbb{R}^{n\times 1}$. Thus, using this approach the original profile constraints (Eq. (20)) in the optimization problem, Eqs. (18-20), can be replaced by the constraints given as

$$[\boldsymbol{\chi}_{\max}(k+1), \boldsymbol{\chi}_{\min}(k+1)] = \widetilde{\mathbf{g}}(\boldsymbol{\chi}(k+1)) \quad (26)$$

$$\mathbf{X}_L \leq \boldsymbol{\chi}_{\min}(k+1), \boldsymbol{\chi}_{\max}(k+1) \leq \mathbf{X}_H \quad (27)$$

Here, Eq. (26) refers to the nonlinear constraint where the function $\widetilde{\mathbf{g}}(.)$ will be used to obtain $\boldsymbol{\chi}_{\max}(k+1)$ and $\boldsymbol{\chi}_{\min}(k+1)$. The solution of optimization problem (Eq. (18)) with constraints given by Eqs. (19), (26) and (27) will result in the estimated states at the collocation points such that the reconstructed spatial profile ($\widehat{\chi}_r(z,k) : r = 1,2,..,n$ and $\forall z \in [0,1]$) will satisfy the specified bounds. Note that unlike the approach proposed by Seth et al. (2023) this approach provides an exact reformulation of the original profile constraints given by Eq. (20). Additionally it guarantees that the estimated profile will fall within the specified bounds. However, due to the root finding step, this approach involves nonlinear constraints and can result in computationally complex nonlinear programming (NLP) optimization problem.

4.2 Using Bernstein Coefficients

Profile constraints satisfaction can also be achieved by expressing state profiles in the form of Bernstein polynomials (BP) and utilising a key property of the BP. Consider the reconstructed state profile for the r^{th} state variable at k^{th} sampling instant, $\chi_r(z,k)$. Note that $\chi_r(z,k)$ represents a N^{th} degree polynomial which can be written as linear combination of coefficients ($c_{r,p}(k)$) and the Bernstein basis ($B_{p,N}(z)$) as (Lane and Riesenfeld (1981)):

$$\chi_r(z,k) = \sum_{p=0}^{N} c_{r,p}(k) B_{p,N}(z) \quad (28)$$

$$\text{where, } B_{p,N}(z) = \binom{N}{p} z^p (1-z)^{N-p} \quad (29)$$

Let $\chi_{r,\max}(k)$ and $\chi_{r,\min}(k)$ denote the maximum and minimum values of the profile $\chi_r(z,k)$ at k^{th} sampling instant over the domain $z \in [0,1]$. An important property of BPs is (Lane and Riesenfeld (1981)):

$$\min_{0\leq p\leq N} c_{r,p}(k) \leq \chi_{r,\min}(k) \leq \chi_{r,\max}(k) \leq \max_{0\leq p\leq N} c_{r,p}(k) \quad (30)$$

The proposed idea is to now represent spatial state profiles as BPs and impose bound constraints on the coefficients of resulting BPs. In view of Eq. (30), this approach will guarantee bound constraints satisfaction by state profiles. This is discussed next.

Defining a matrix of Bernstein basis evaluated at collocation points (ξ_j) as:

$$\mathcal{B} = \left[\left(\mathcal{B}^d\right)^T \ \left(\mathcal{B}^a\right)^T \right]^T_{(N+1)\times(N+1)}$$

$$\text{where, } \mathcal{B}^d = \begin{bmatrix} B_{0,N}(\xi_2) & \cdots & B_{N,N}(\xi_2) \\ \vdots & \ddots & \vdots \\ B_{0,N}(\xi_N) & \cdots & B_{N,N}(\xi_N) \end{bmatrix} \quad (31)$$

$$\text{and} \quad \mathcal{B}^a = \begin{bmatrix} B_{0,N}(\xi_1) & \cdots & B_{N,N}(\xi_1) \\ B_{0,N}(\xi_{N+1}) & \cdots & B_{N,N}(\xi_{N+1}) \end{bmatrix} \quad (32)$$

and a vector of coefficients for r^{th} state profile as:

$$\mathcal{C}_r(k) = \left[\, c_{r,0}(k) \ \cdots \ c_{r,1}(k) \ \cdots \ c_{r,N}(k) \,\right]^T_{(N+1)\times 1} \quad (33)$$

The state vector for r^{th} state variable can be written as

$$\boldsymbol{\chi}_r(k) = \left[\left(\boldsymbol{\chi}^d_r(k)\right)^T \ \left(\boldsymbol{\chi}^a_r(k)\right)^T \right]^T = \mathcal{B}\mathcal{C}_r(k) \quad (34)$$

Further, stacking the above quantities as:

$$\mathbb{B}^d = blockdiag(\mathcal{B}^d, ..., \mathcal{B}^d, ..., \mathcal{B}^d) \quad (35)$$

$$\mathbb{B}^a = blockdiag(\mathcal{B}^a, ..., \mathcal{B}^a, ..., \mathcal{B}^a) \quad (36)$$

$$\mathbb{C}(k) = \left[\, (\mathcal{C}_1(k))^T \ \cdots \ (\mathcal{C}_n(k))^T \,\right]^T_{n(N+1)\times 1} \quad (37)$$

the augmented state vector can be represented as

$$\boldsymbol{\chi}(k) = \mathbb{B}\mathbb{C}(k) \quad (38)$$

$$\text{with } \mathbb{B} = \left[\left(\mathbb{B}^d\right)^T \ \left(\mathbb{B}^a\right)^T \right]^T_{n(N+1)\times n(N+1)} \quad (39)$$

Thus, using the relationship given by Eq. (38) and the property of BP given by Eq. (30) the bounds on the estimated profiles can be imposed by constraining the predicted coefficients for individual state variables. Thus, Eq. (20) representing the profile constraints in the constrained update step (Eqs. (18) to (20)) can be replaced by

$$\mathcal{X}_L \leq \mathbb{C}(k) = \mathbb{B}^{-1}\boldsymbol{\chi}(k) \leq \mathcal{X}_H \quad (40)$$

where, $\mathcal{X}_L$ and $\mathcal{X}_H \in \mathbb{R}^{n(N+1)\times 1}$ are the vectors containing the lower and upper bounds for the state profiles of various state variables as

$$\mathcal{X}_L = \left[\, (x_{1,L})\, \mathbf{1}^{N+1} \ \cdots \ (x_{n,L})\, \mathbf{1}^{N+1} \,\right]^T \quad (41)$$

$$\text{and } \mathcal{X}_H = \left[\, (x_{1,H})\, \mathbf{1}^{N+1} \ \cdots \ (x_{1,H})\, \mathbf{1}^{N+1} \,\right]^T \quad (42)$$

Here, $\mathbf{1}^{N+1}$ represents row vector of ones of size $(N+1)$. Note that Eq. (40) represents linear inequality constraints.

Table 1. Comparison of various approaches for constrained profile estimation

Approaches	Discretization based (Seth et al. (2023))	Extremum based (Current work)	BP based (Current work)
Relation to original prob.	Approx. reformulation (less conservative)	Exact reformulation	Approx. reformulation (more conservative)
Nature of optim. prob. (DAEs with linear algb. eqns.)	QP	NLP	QP
Constr. satisf. guarantee	No	Yes	Yes

Table 2. Modeling related parameters

	Plant(FD model)	OC model
No. of grid/colloc. points	501	13
No. of differential states	998	22
No. of algebraic states	4	4
Size of state vector	1002×1	26×1
No. of temp. measurements	6	6

Further, it is to be noted BP based approach is conservative in nature. This is because constraining the coefficients ensures bounded estimated state profiles, but violation of bounds by Bernstein coefficients does not necessarily imply that estimated state profiles will also violate the bounds. For the special case of linear algebraic constraints, BP based approach leads to a QP problem. The existing and proposed approaches are compared in Table (1).

5. CASE STUDY

5.1 *Auto-thermal rector system*

We now investigate the effectiveness of our proposed approaches in generating accurate state profile estimates that satisfy specified bounds on a simulation based Auto-Thermal tubular reactor system with two primary state variables: dimensionless concentration (C) and dimensionless temperature (T). The coupled PDEs governing the pseudo homogeneous dynamic model of the system are given in Berezowski et al. (2000). Simulations are based on the parameter values provided by Pacharu et al. (2012): $Pe_m = 100$; $Pe_T = 100$; $\delta = 2$; $\psi = 0.3$; $Da = 0.15$; $\kappa = 2$; $\gamma = 10$; $\omega = 1.4$. Further details on the order of plant ('FD model') and the chosen OC model for developing state estimator are summarized in Table (2). Also note that the matrices ($\mathbf{Q}_a, \mathbf{R}_a$ and $\mathbf{S}$) corresponding to the model plant mismatch (MPM) are evaluated once the order of the OC model is fixed. For more details on these aspects refer Seth et al. (2023). For estimation purposes, the initial covariance corresponding to differential states, $\mathbf{P}^d_{0|0}$ was taken as $3\mathbf{I}_{22\times22}$. Temperature measurements at 6 equidistant locations were assumed to be available $(0, 0.2, 0.4, 0.6, 0.8, \text{and } 1)$ units. The measurements were assumed to be corrupted with sensor noise, $\mathbf{R}_s = 0.01^2 \times \mathbf{I}_{6\times6}$. The cooling medium in the jacket was treated as the manipulated input, $T_H(k) = T_{H,m}(k) + \mathbf{w}_u(k)$ where, $\mathbf{w}_u(k) \sim \mathcal{N}(0, \mathbf{Q}_u)$ and $T_{H,m}(k)$ varies as a multistep input signal with $\mathbf{Q}_u = 0.001^2$.

The following approaches are compared:
Approach A: Profile constraints imposed using discretization based approach (ref: section (3.2)).
Approach B: Profile constraints approach based on the extremum of the estimated state profiles.
Approach C: Profiles constraints approach based on the Bernstein coefficients.
Note that the constrained update step is invoked only when there is violation of constraints. For approaches B, and C, this violation was checked by checking the profile extremes as discussed in Section (4.1), while for approach A the violation was checked by checking constraints violation at the discretized points.

State estimation was performed for $M = 30$ stochastic simulation runs, and $N_s = 150$ sampling instants. The stochastic simulations vary in initial state profiles to the plant, manipulated input sequence and the noise realizations in measurements and disturbance inputs. Figure (1) shows the snapshots of profile estimates of reactor concentration for a typical simulation run. For illustrative purposes, we have also included the profile estimates obtained with bounds imposed only on the state values at collocation points (conventional approach). It can be seen that the approaches A-C prevent the violation of constraints by the estimated profiles. The performance

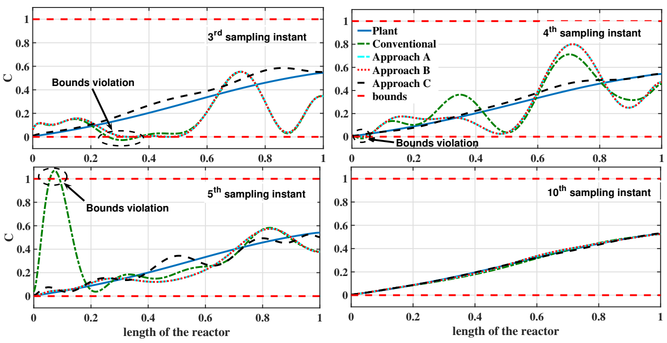

Fig. 1. Profile estimates of concentration at initial sampling instants for various approaches

of approaches A-C are further examined using average normalized root mean square error (ANRMSE) computed for r^{th} state as:

$$\text{ANRMSE}_r = \frac{1}{MN_s}\sum_{p=1}^{M}\sum_{k=0}^{N_s}\text{NRMSE}_r^{(p)}(k) \quad (43)$$

where, NRMSE stands for normalized root mean squared error values. For the p^{th} simulation run it is defined as:

$$\text{NRMSE}_r^{(p)}(k) = \frac{1}{\sigma(\mathbf{X}_r^{(p)}(k))}\left[\frac{\sum_{i=1}^{N_f+1}(\varepsilon_r^{(p)}(z_i,k))^2}{N_f+1}\right]^{\frac{1}{2}} \quad (44)$$

$$\text{where, } \varepsilon_r^{(p)}(z_i,k) = x_r^{(p)}(z_i,k) - \widehat{\chi}_r^{(p)}(z_i,k|k)$$

Here $\mathbf{X}_r^{(p)}(k)$ is the plant profile vector of r^{th} state variable obtained at k^{th} sampling instant of p^{th} simulation run, $\sigma(.)$ represents the standard deviation in the corresponding state profile, $x_r^{(p)}(z_i,k)$ and $\widehat{\chi}_r^{(p)}(z_i,k|k)$ are the plant and estimated values of the state evaluated for the i^{th} grid point at k^{th} sampling instant of p^{th} simulation run. $N_f + 1$ is the total number of FD grid points. The mean of the square of errors throughout the spatial profile of the reactor was evaluated at k^{th} instant and was normalized by the variance in the true profile at that instant. Also, mean average profile squared error (MAPSE) values were evaluated to compare the profile estimation errors. MAPSE values for the r^{th} state variable is defined as:

$$\text{MAPSE}_r(z_i) = \frac{1}{M}\sum_{p=1}^{M}\left(\frac{1}{N_s}\sum_{k=1}^{N_s}\left(\varepsilon_r^{(p)}(z_i,k)\right)^2\right) \quad (45)$$
$$0 \leq z_i \leq N_f + 1$$

The average computation time per time instant for different schemes is also compared.

Observing the time averaged profile estimation error plotted in Figure (2) it can be concluded that out of the three approaches, imposing constraints using Bernstein coefficients produces profile estimates with low estimation error throughout the spatial domain. On the other hand, setting constraints using the extreme values of the profiles can lead to high estimation errors. The ANRMSE and the

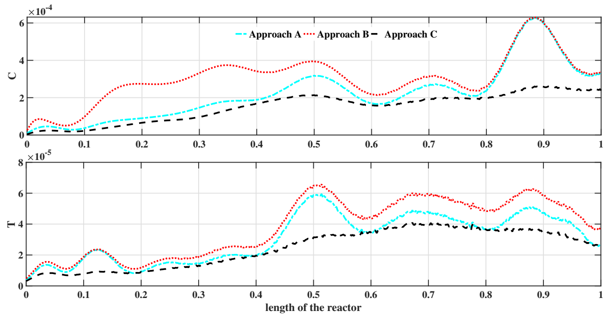

Fig. 2. MAPSE for various estimation schemes

avg. computation time for the 30 stochastic simulations are stated in Table (3). The values in the bracket are evaluated considering only first 20 sampling instants where constraint violations are more prominent. The values presented in Table (3) demonstrate significant difference in computational efficiency among three different approaches. Specifically, the approach utilizing Bernstein coefficients is approximately 8 and 16 times faster than root-finding, and spatial discretization approaches, respectively. This is because Bernstein coefficient approach involves solving QP with only a few linear inquality constraints. Further, it is important to note that the quality of profile estimates and the computation time for the spatial discretization based approach depends on number of discretization points used for imposing profile constraints. It is evident from the estimation error values that the use of extreme values of the polynomials for constraint satisfaction leads to notably higher estimation errors. On the other hand, the approach utilizing Bernstein coefficients outperforms the other two approaches in terms of profile estimation accuracy.

6. CONCLUSIONS

Two analytical methods for constrained profile estimation of DPSs are proposed. In particular, the constrained

Table 3. ANRMSE and comp. time values

	Approach-A	Approach-B	Approach-C
ANRMSE-C	0.0261	0.0315	**0.0234**
ANRMSE-T	0.0393	0.0458	**0.0361**
Avg. comp. time (sec)	0.0659 (0.3559)	0.0419 (0.1678)	**0.0224 (0.0215)**

update step for EKF was modified to account for the constraints on the spatial profiles over the entire spatial domain. The modifications ensure that the state profiles reconstructed using estimated OC state vector are bounded. The first method involves finding and constraining the maximum and minimum values of the spatial profiles in the relevant spatial domain of the system. This approach leads to the formulation of nonlinear programming problem (NLP), due to the nonlinear computations required for determining extremum values of the approximated polynomials. The second approach leverages the property of the Bernstein form of polynomials and thus requires the representation of the spatial state profiles in Bernstein from. Here, bounds are imposed indirectly by constraining the coefficients of the Bernstein polynomials, thereby resulting in conservative bounds. However, this method allows the formulation of bounds as linear inequality constraints. Thus this approach is computationally efficient as compared to the former approach as depicted from the average computational time values obtained in the case studies. The results from simulation studies conducted on tubular reactor system demonstrates the efficacy of the proposed methods in producing spatial state profiles within the specified bounds.

REFERENCES

Berezowski, M., Ptaszek, P., Jacobsen, E. W., 2000. Dynamics of heat-integrated pseudohomogeneous tubular reactors with axial dispersion. Chemical Engineering and Processing: Process Intensification 39 (2), 181–188.

Gupta, S. K., 1995. Numerical methods for engineers. New Age International.

Lane, J. M., Riesenfeld, R. F., 1981. Bounds on a polynomial. BIT Numerical Mathematics 21 (1), 112–117.

Mandela, R. K., Rengaswamy, R., Narasimhan, S., Sridhar, L. N., 2010. Recursive state estimation techniques for nonlinear differential algebraic systems. Chemical engineering science 65 (16), 4548–4556.

Marko, L., Mennemann, J.-F., Jadachowski, L., Kemmetmüller, W., Kugi, A., 2018. Early-and late-lumping observer designs for long hydraulic pipelines: Application to pumped-storage power plants. International Journal of Robust and Nonlinear Control 28 (7), 2759–2779.

Pacharu, S. R., Gudi, R., Patwardhan, S., 2012. Advanced state estimation techniques for packed bed reactors. IFAC Proceedings Volumes 45 (15), 519–524.

Seth, G., Patwardhan, S. C., Bhushan, M., 2023. Constrained profile estimation for distributed parameter system in one dimension using orthogonal collocation. Journal of Process Control 128, 103011.

Yupanqui Tello, I. F., Vande Wouwer, A., Coutinho, D., 2021. A concise review of state estimation techniques for partial differential equation systems. Mathematics 9 (24), 3180.